GUN TUBE SURFACE KINETICS AND IMPLICATIONS

Paul J. Conroy[1], Michael J. Nusca[1], Cary Chabalowski[1], William Anderson[1]

[1]*U.S. Army Research Laboratory, Aberdeen Proving Ground, MD 21005-5066*

Current theories concerning gun tube erosion consider that erosion can occur under various conditions. Propellant product gases are known to react with the surface resulting in an altered surface material which may melt or pyrolyze due to a lower melting temperature than that of the gun steel and or weakened mechanical properties. Previous surface reaction studies by the authors used a generalized equilibrium scheme with a control volume analysis to represent surface reactions occurring during a cannon firing. This led to a post reaction treatment at the interface which incorporated the subsurface diffusion of species to limit the surface reaction. In this study, the surface reactions and rates are specified explicitly with published rates and guidance from fundamental molecular modeling results. The results demonstrate the utility of the employed surface reaction mechanism as well as the incorporation of finite rate surface kinetics.

INTRODUCTION

In consideration to the development of the Future Combat System, it is necessary to understand the physics and chemistry of the interior ballistic erosion problem in order to focus mitigation efforts. This current study focuses upon the incorporation/application of generalized finite rate kinetics to the gun tube erosion problem. Previously, there has been documented a melt wipe model by Weinacht, Conroy, [1], and Conroy, Weinacht, Nusca [2], followed by the inclusion of generalized equilibrium of Conroy, Weinacht, Nusca, [3], [4], and [5]. The melt-wipe description enabled very severely eroding systems to be modeled. However, it did not account for the erosion in systems which apparently did not reach the melting temperature of the gun steel. These systems at the time were thought to have some form of augmented heat transfer due to projectile blowby [6], or heat release at the surface due to chemical reactions. It was initially thought that the oxidation of the surface was releasing sufficient energy to melt the oxidized material. This material along with its energy was subsequently blown out of the gun tube in the product gases. Thus the tube effectively did not experience any additional heating as might be evidenced experimentally. Chemical phenomena were investigated initially due to unusual behavior of RDX containing propellants. The adiabatic flame temperature of M43, which contains RDX, is lower than that of M30,which does not contain RDX, while the erosivity was typically higher [7]. This behavior conflicts with previously held beliefs and correlations which used the flame temperature to identify erosivity [8], [9], and [10]. Possible causes for this behavior were hypothesized after the inclusion and application of equilibrium chemistry to the erosion problem [5]. The equilibrium chemistry required the definition of a specific control volume for the reaction which was defined by the diffusion depth of carbon into the surface. The

premise was that no more steel could react with carbon or oxygen than that in physical contact with the gaseous atomics. Therefore the limiting factor was diffusion.

Although equilibrium chemistry continues to be applied for reaction of materials which diffuse into the substrate in the present work, the inclusion of finite rate kinetics at the surface has resulted in an elimination of many of the assumptions from the equilibrium calculations. Finite rate kinetics also allows the inclusion of many erosion reaction inhibition concepts which can lead or direct investigations of mitigating additives or chemical surface alterations.

PHYSICAL DESCRIPTION

Figure 1 describes the physical result of gun firings on a coated gun tube. The cracks inherent in the chromium plating, produced by either residual stresses from the manufacturing process or from thermo-mechanical cycling during gun firings, enable gases to reach the substrate where they react with the surface altering it from virgin gun steel. This altered surface is much easier to remove either through pyrolysis or melting. A critical description of the loss of surface coatings was pointed out by Conroy, Weinacht, and Nusca, [5], namely in that the erosion preferentially traverses laterally under the coating following the conductive energy transported through the coating to the substrate. Thus the interface between the substrate and the surface material is the hottest location at the bottom of the pit or crack and therefore the most reactive. This causes coating undermining and subsequent removal by high pressure gas in this region after the passage of the rarefaction wave during gun tube blowdown.

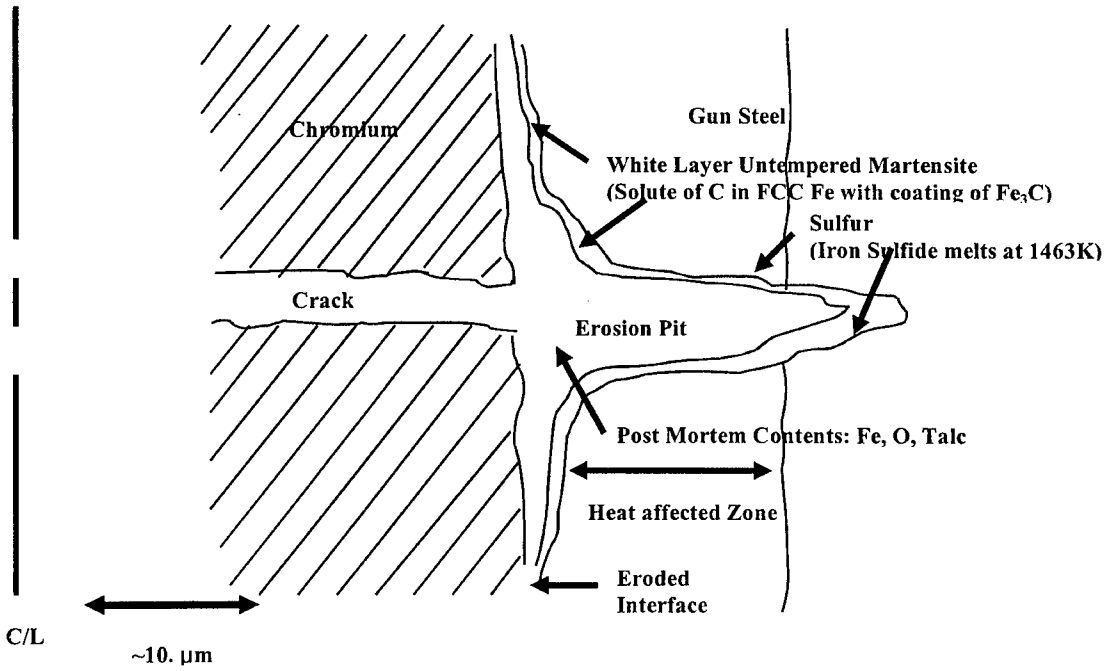

Figure 1. Description of Post Mortem Erosion Pit [19].

Figure 2 describes the physical representation that has been incorporated into the erosion model. Included in the figure and representation are the core flow species which supply both heat and mass transfer to the surface. Stresses are considered in both the coating as well as the substrate. This stress results from both the surface boundary condition of pressure as well as the mismatch in coefficients of thermal expansion between the coating and substrate. When the stress in the coating exceeds the ultimate strength a crack is assumed to form. This produces a crack distribution within the coating. Excessive interfacial shear stress would cause the coating to delaminate and subsequently be removed. Convective heat transfer imparts energy to the surface of the coating as well as in the crack where it is augmented. Energy is transported through both the coating and substrate material. Further details are described in previous reports [3], and [5].

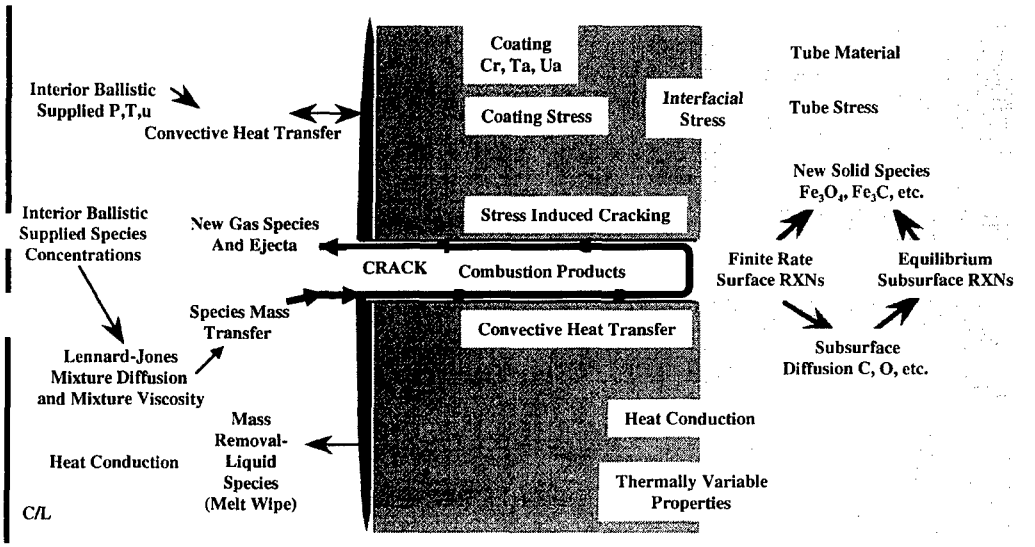

Figure 2. Analytical Description Including Kinetics and Coatings.

Surface kinetics have been included in the following manner. The species transported down into the crack are determined through multi-component diffusion with Wilke's [11] mixing rule to account for interactions. The quantity of surface iron available for reaction remains determined from the thermally variable diffusion depth for carbon over the computational time step at the crack base surface temperature where alpha is the diffusivity and dt is the time-step. The reaction mixture temperature is determined through a weighting function between the gas and solid phase materials. Given the specific heats, average molecular weight, identity and quantity of reactants along with user supplied reactions such as provided in Table 3, the nonequilibrium kinetic subroutine models the reaction of the species through the macroscopic hydrodynamic time-step. By specifying the maximum kinetic time-step, which is much smaller than the hydrodynamic time-step, to at least 1/25 but no more than 1/500 iterations per hydrodynamic time step enables the product species from one kinetic computational sweep through the reaction mechanism to interact as reactants for all the other reactions in the mechanism.

When the kinetics routine calculation is completed for the hydrodynamic time-step the integrated quantity of carbon and oxygen which diffused into the steel from the dissociation of CO is subsequently reacted with the substrate through equilibrium chemistry as guided from previous work with the model. In the current model binary diffusion of species into the solid phase is assumed. This approach does not account for cross terms of additional species. Inclusion of full multi-component subsurface diffusion is planned as a future effort. The quantity of material diffused appears to be small in comparison to the surface reacting material, although during the cooling portion of the ballistic cycle the diffusion continues for quite some time after the surface passes the melting temperature of Fe_3C. The period of time between the time when the interface temperature decreases below the melting temperature of Fe_3C and the time when the temperature at which diffusion stops is reached is what potentially makes diffusion important. During this time material is being inserted through diffusion into the steel and the following shot will encounter a loaded substrate which will be removed.

Once both the surface and subsurface systems have reacted the post reacted products are prepared for carry over to the next time-step. This step allows for the determination of energy released positive or negative as well as the surface material lost or gained. This energy is incorporated as a surface source term.

NONEQUILIBRIUM CHEMICAL KINETICS

The nonequilibrium (or finite-rate) chemical kinetics subroutine has been adapted from the NSRG computational fluid dynamics code written at ARL [12], and recently applied to propulsive reacting flow systems [13] as well as an open-air, high-speed chemically reacting jet [14]. In the NSRG code, this subroutine is used to compute the chemical source term that appears on the right-hand side of each species conservation equation in the Navier-Stokes equation set. For use in the present effort, this subroutine has been adapted so that it is patterned after the equilibrium subroutine, documented previously [5]. As a result, the Army Research Laboratory Erosion Code, (ATEC) determines the local flow conditions (density, temperature, and species mass fractions) and numerical conditions (time step or interval) while the nonequilibrium subroutine (using an appropriately smaller chemical time step) returns the new chemical constituency based on a predetermined set of chemical reactions and rates (i.e., the chemical mechanism). In this section a general review of the nonequilibrium routine is given.

Chemical reactions can be expressed in a general fashion (where X_i represents the symbol for species i, for example H_2O) with stoichiometric coefficients, ν, for each species in these reactions.

$$\sum_{i=1}^{N} \nu_i' \, X_i \; \Leftrightarrow_{k_b}^{k_f} \; \sum_{i=1}^{N} \nu_i'' \, X_i \tag{1}$$

A chemical kinetics mechanism will consist of L such reactions. For each reaction a general reaction rate equation is written.

$$\frac{dC_i}{dt} = \sum_{i=1}^{L} (\nu_i'' - \nu_i') \left(k_f \prod_{i}^{N} C_i^{\nu_i'} - k_b \prod_{i}^{N} C_i^{\nu_i''} \right) \tag{2}$$

where the C_i above represents the concentration of species i. This equation relates the time rate of change of this concentration for a particular species (the left-hand side) to the current values of concentrations for all N species, raised to powers of either the reactant coefficient (ν-prime) or product coefficient (ν-double-prime). In Equation 2, the reaction rates (k) and the stoichiometric coefficients for the reaction (ν) multiply the product sums. In order to compute the total change in C_i this equation represents a sum over every reaction (total of L) in the reaction mechanism. The nonequilibrium routine determines the largest physical time step (dt in Equation 2) which is also smaller than the fluid time step from ATEC and computes the new species concentrations (using dC_i/dt) for all N species. Concentrations can be converted to mass fractions for convenience. In general, tens or hundreds of chemical time steps will have to be taken per one fluid time step (see [11], for more details).

The forward reaction rate is usually defined using the Arrhenius form,

$$k_f = \mathrm{A}\, T^{\mathrm{n}} \exp(-E_a / \mathrm{k}T) \tag{3}$$

where the rate data: A, E_a and n are determined from physical chemistry (k is Boltzmann's constant and is used to express E_a/k in temperature units). The backward rate can either be specified in the same form as the forward rate (above) or can be computed using the equilibrium constant for each reaction,

$$k_b = k_f / K_c \;\; ; \;\; K_c = \exp\left(-\Delta G / RT\right) \tag{4}$$

where K_c is the equilibrium constant for a particular reaction computed from the change in Gibbs energy (ΔG) for that reaction (see [12] for details). Gibbs energy for each species is computed using the NASA-Lewis database [15].

There are many situations for which reaction rates are of the additive type (wherein two rates are computed and added together for the final rate) or the pressure dependant "falloff" type (wherein the final rate is the product from three factors; two separate rates and a function based on the local flowfield temperature, pressure and mixture). The nonequilibrium routine will accept special coding for these cases. In other situations, certain reactions involve a "third-body" or a "collision partner" (often denoted M). The species M can stand for any of the N species being considered in the mechanism; thus a single reaction involving M-type species is actually N reactions with the same reaction rate. For these N reactions, there is usually specified a third-body collision efficiency for a particular collider species. These efficiency factors are multiplied by the concentration of the collider species in the product-summation terms of Equation 2. The nonequilibrium routine is setup to automatically handle third-body reactions. For an example of these situations (i.e., non-Arrhenius reaction rates and third-body reactions) the reader is directed to [14].

CHEMICAL KINETICS MECHANISM

A finite rate chemical reaction module has been incorporated into the erosion package as described. Before proceeding to use the package a series of numerical experiments were made to insure that the correct information was passed to and returned from the module. One the numerical validating experiments involves a simple set of reactions to test various areas

of kinetics involving both temperature sensitivity as well as possible third body reactions, presented in Table 1.

Table 1. Example Kinetics Validation Reaction Set.

Reaction		A (cm^3/mole s) or (cm^6/$mole^2$-s)	n (-)	E_a/k (K)	3rd Body
1	H_2 (g) + O_2 (g) ⇒ 2OH (g)	1.7e13	0.0	24169.	no
2	OH (g) + H_2 (g) ⇒ H_2O (g) + H	2.2e13	0.0	2593.	no
3	OH (g) + H (g) ⇒ H_2O (g)	2.2e22	-2.0	0.0	Yes

Table 2 describes the results for the validation kinetic reaction calculation, presented in Table 1, using the module as a stand alone package which has been extensively tested (Nusca 1998) and the integrated version of the module in the erosion package. Both the stand alone and integrated versions produce identical results without the reverse reactions. However, if the reverse reactions are enabled then the integrated package depends upon the older version of the NASA Lewis database which is automatically read in, while the stand alone package uses a newer NASA Lewis database. The differences observed with the reverse calculations implemented is due to versions of the thermochemical database. If this ultimately causes large discrepancies, the older database could be updated, however, the effect appears to be orders of magnitude smaller than what would be considered an issue.

Table 2. Mass Fraction Production Rates for Kinetics Validation Reaction Set.

Integrated Kinetics (With and without backward reactions)			Stand Alone Kinetics Module (With and without backward reactions)		
SPECIES	g/cm^3-s		SPECIES	g/cm^3-s	
1	-0.16962E+05	H	1	-0.16962E+05	H
2	0.00000E+00	H_2	2	0.00000E+00	H_2
3	0.00000E+00	O_2 Without	3	0.00000E+00	O_2 Without
4	-0.28622E+06	OH Backward	4	-0.28622E+06	OH Backward
5	0.30318E+06	H_2O Rate	5	0.30318E+06	H_2O Rate
1	-0.16962E+05	H	1	-0.16962E+05	H
2	0.18858E+00	H_2	2	0.19973E+00	H_2
3	0.29935E+01	O_2 With	3	0.31805E+01	O_2 With
4	-0.28623E+06	OH Backward	4	-0.28623E+06	OH Backward
5	0.30318E+06	H_2O Rate	5	0.30318E+06	H_2O Rate

A proposed set of reactions between the primary propellant combustion products (H_2, CO, CO_2, H_2O) with the surface of the gun tube BCC, FCC iron is presented in Table 3. Although the reverse reactions could have been included at this time only the forward reactions are considered. The coefficients and exponents in Table 3 are literature values except for the coefficient of reaction number 2 which was not available from the literature. Fortunately the exponent for reaction number 2 was available. This provided a starting point from which to develop some estimates for the coefficient. A parametric study involving

many calculations was performed on the coefficient, a few of which are presented in Figure 3. As the coefficient A_2 is increased from 3.8e14 to 6.0e14 what is immediately clear is the effect of reaction temperature and duration on pit growth. This modification affects the quantity of material removed in the forcing cone region. Farther down-bore there is a gradual asymptote to a common amount of material removed.

Table 3. Proposed Reaction Mechanism

	Reaction	A (cm^3/mole-s) or (cm^6/$mole^2$-s)	n (-)	Ea/k (K)	3rd Body
1	$CO(g) + O(ads) + (Surface) \Rightarrow CO_2(g) + (Surface)$ [16]	6.17e14	0.0	1510.0	Yes
2	$CO(g) + (Surface) \Rightarrow C(ads) + O(ads) + (Surface)$ [17] (Collider)	5.2e14 (Estimate)	0.0	23903.0	No
3	$O(ads) + O(ads) + (Surface) \Rightarrow O_2(g) + (Surface)$ [16]	1.89e13	0.0	-900.0	Yes
4	$H(g) + OH(ads) + (Surface) \Rightarrow H_2O(g) + (Surface)$ [16]	8.35e21	-2.0	0.0	Yes
5	$H_2(g) + (Surface) \Rightarrow 2H(g) + (Surface)$ [16]	4.57e19	-1.4	52530.0	No
6	$H(g) + O(ads) + (Surface) \Rightarrow OH(ads) + (Surface)$ [16]	4.71e18	-1.0	0.0	Yes
7	$CO(g) + O_2(ads) + (Surface) \Rightarrow CO_2(g) + O(ads) + (Surface)$ [16]	5.06e13	0.0	31800.0	No

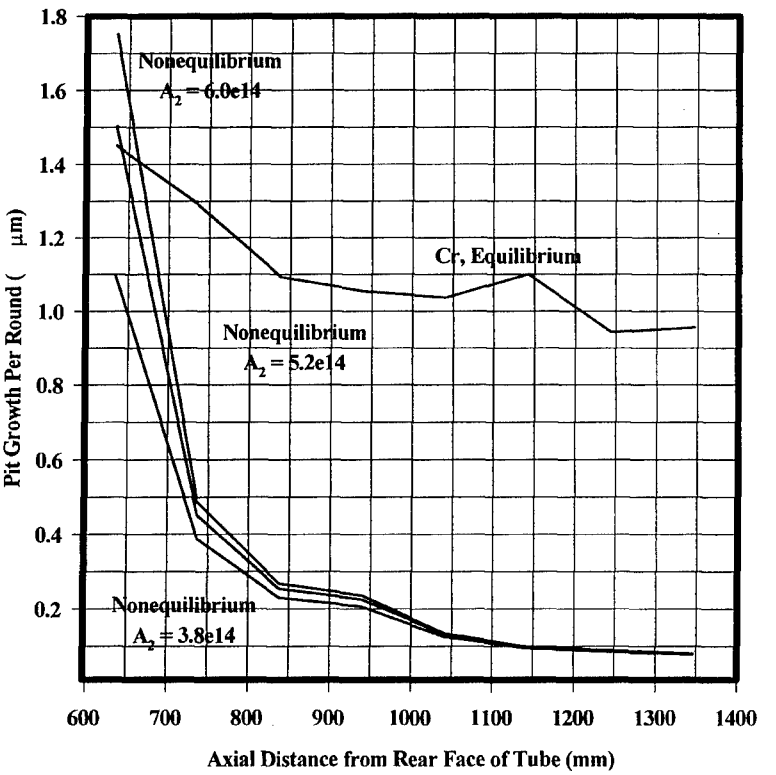

Figure 3. Pit Growth Rate for Chrome Coated Steel 120mm, M256 Canon Firing and APFSDS Round with Various Reaction Rate Coefficients.

A substantial difference exists between the previous calculation using infinite rate (equilibrium) chemistry and the finite rate chemistry results. The previous results do not take reaction rates into account and therefore the pit growth rate results are much higher down-bore than they apparently should be. The chemical reaction rates control the amount of product formed as well as the supply of potential reactants for intermediate reactions. The depth of material typically removed from the base of a pit is between 0.7μ and 1.5μ per shot for this particular APFSDS round [19]. This magnitude is verified by micrographs [20], such as shown in Figure 4. This leads to assignment of 5.2e14 to the coefficient value A_2. Whether this assigned value is correct or not is purely speculation at this time. One item which the equilibrium calculations provided is the resultant chemical constituency involving iron carbide. Therefore, the resultant carbon, from reaction number 2 in Table 3, was enabled to react with the iron at the surface to produce iron carbide.

RESULTS

Figure 5 compares the previous equilibrium assumption to the present nonequilibrium assumption for a 0.010" chromium plated M256 120mm tank canon firing an APFSDS round.. Also presented is data from a M68 non chromed tank cannon firing a similar round but reduced by a factor of ten (Ward, 1980). The difference in predictions between the equilibrium and nonequilibrium assumptions is striking. The equilibrium assumption produces more erosion down-bore than the nonequilibrium assumption. Closer to the forcing cone for the M68 data as well as the nonequilibrium calculation we see that the higher temperatures guide the reaction rate. Although the nonequilibrium resultant eroded depth should be less than that of the equilibrium this is not necessarily the case since the computational scheme is somewhat different between the two. The equilibrium scheme was based on a fixed control volume with a finite amount of iron, while the nonequilibrium scheme enables iron to be consumed as needed by the surface reaction.

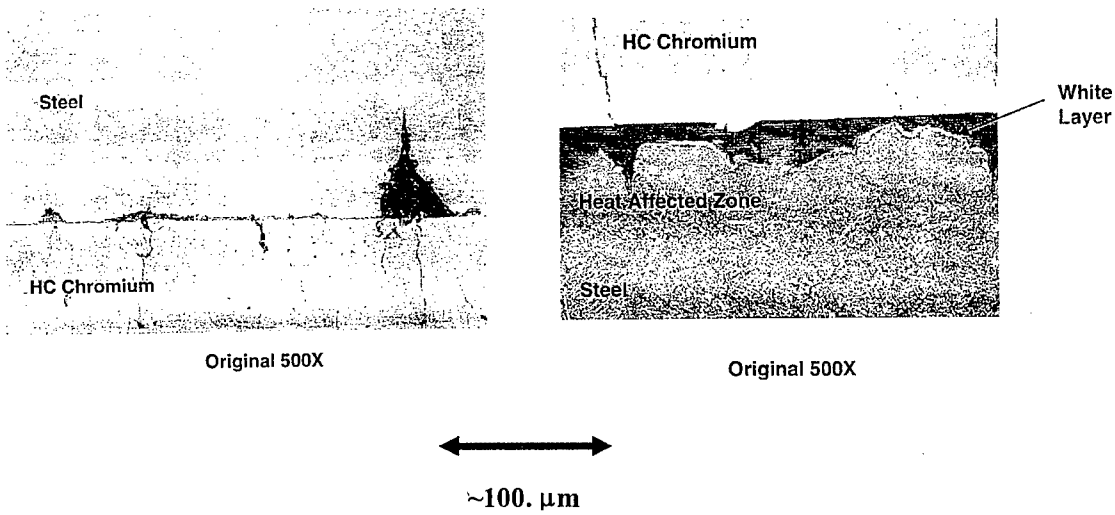

Figure 4. Substrate Erosion Beneath Cracks Showing Lateral Erosion Distribution [20].

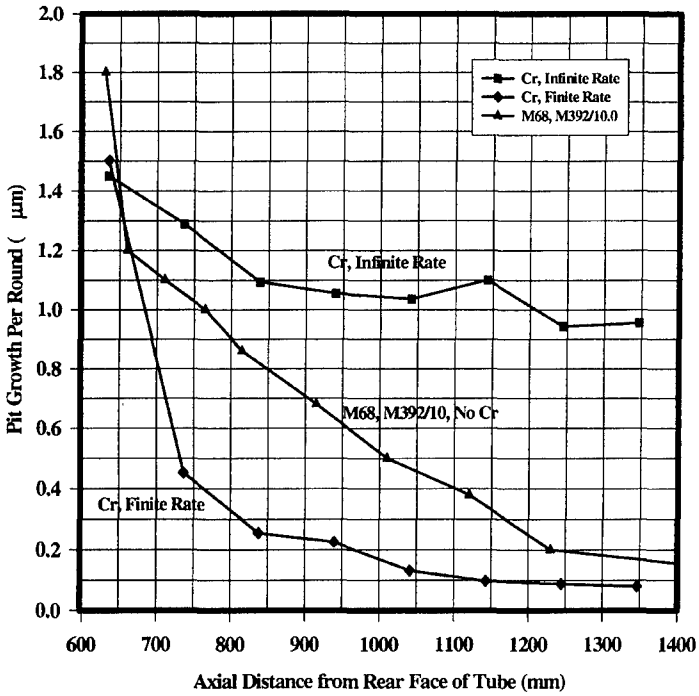

Figure 5. Single Firing Pit Growth Rate for 0.010" Chrome Plated Steel Compared to M68 Non-Chromed Gun Firing an M392/10. APSFDS Round.

Using the previously determined value for A_2, calculations for a similar tantalum coating were made and presented in Figure 6. The only modifications were to the physical properties of tantalum. Figure 6 also compares equilibrium as well as non equilibrium results for both chromium as well as tantalum coated tubes. The large difference in the potential pit growth rate at the forcing cone, between Cr and Ta, is due to the inherent higher temperature experienced with the tantalum coating as seen in Figure 7. The peak temperature experienced by the pit interface is almost 200K higher for the tantalum than that for the chromium. This drives the exponent in the Arrhenius reaction rates as well as the substrate diffusion of the species. This may imply that if there was a crack or other type of pit form given a tantalum coating of equal thickness as chromium then perhaps the tantalum coating would not tend to have the longevity of the chromium coating in similar circumstances.

NITROGEN HYPOTHESIS

Considering that the primary driving reaction of the chemical mechanism is the dissociation of the carbon monoxide, ways to possibly mitigate erosion would include methods to suppress this dissociation or suppress the production of carbon monoxide in the first place. Interestingly, Ponec and Barneveld, [21] suggest that the surface dissociation of CO on an iron surface is spoiled by nitrogen intrusion or nitriding the surface. They do not state specifically why this occurs. This leads to the possibility that increasing the nitrogen content of the propellant products may diminish the CO dissociation and thereby the erosion. Leveritt, Conroy, and Johnson [22] have discovered that some advanced propellants, with similar flame temperatures as older propellants such as JA2, do not erode as much as the older double base propellant. Complicating matters is the fact that these advanced propellants have a much higher CO/CO_2 ratio than that of the double base propellants. One

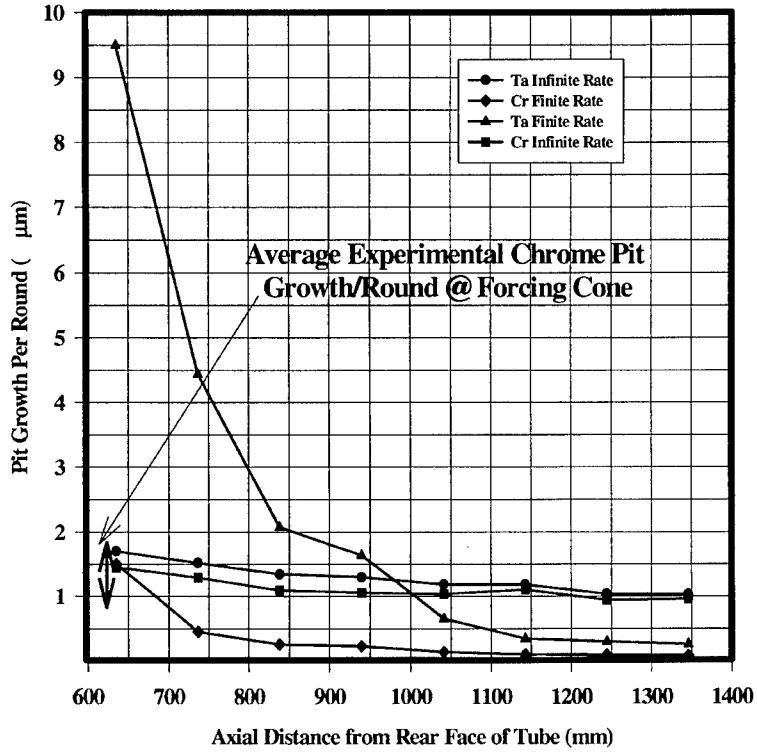

Figure 6. Single Firing Pit Growth Rates for 120mm, M256, Cr and Ta Lined, Firing an APFSDS Round.

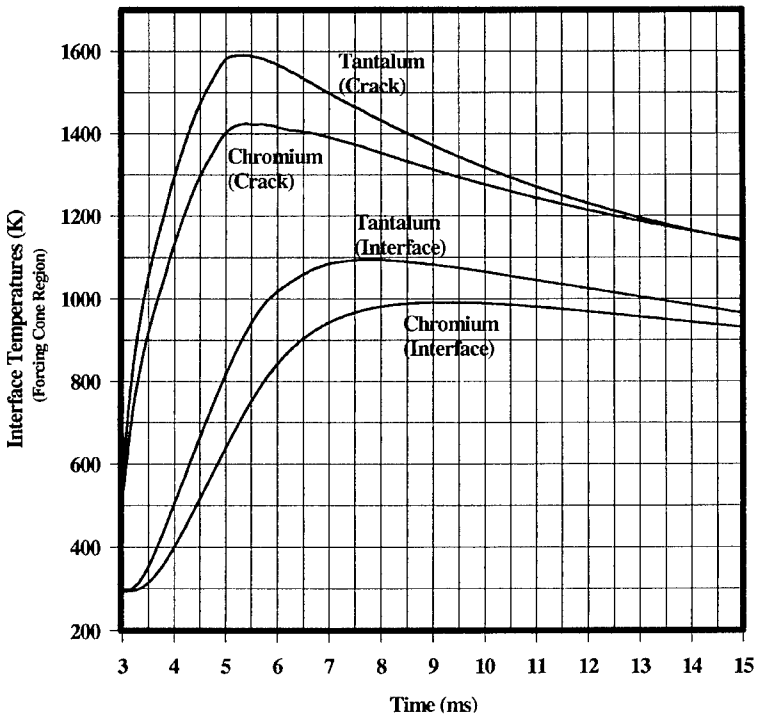

Figure 7. Computed Interfacial Crack Base Temperatures for 0.010" Chromium Coating Compared to 0.010" Tantalum Coated M256 Canon Firing an APFSDS Round.

would expect these higher ratios to exacerbate the carburization mechanism. Fortunately, Ponec's explanation may be applied to these new propellants because their nitrogen content is approximately three times that of conventional propellants.

The M242 Bushmaster barrel has the option of nitriding or chrome plating. If it is chrome plated, access for erosion is through the cracks to the substrate [5]. Considering Ponec's and Barneveld's hypotheses, investigation into nitriding surfaces before they are chrome plated or even afterward may lead to technological breakthroughs to increase the service life by mitigating the erosion at the base of the cracks. It is not believed by the authors at this time that the nitrided chemical process involved for nitriding to mitigate erosion was previously understood, other than that it increased the surface hardness. We now have a possible chemical rationale for nitriding gun barrels in that the nitrogen appears to either interfere with the dissociation of the carbon monoxide on the surface, or perhaps interfere with the diffusion of carbon into the substrate steel.

DISCUSSION

Nonequilibrium chemical kinetics have been incorporated in the erosion calculations. The user may input externally the reaction mechanism desired with standard kinetic rate parameters. For the iron-gas system a potential mechanism was investigated. One reaction coefficient was unknown for the mechanism and was estimated through a parametric study. Fortunately Grabke [17] investigated the specific dissociation of CO on the iron surface and reported the activation barrier. This enabled the inclusion of the reaction while an estimate of the reaction coefficient was made through a parametric study.

Nonequilibrium and equilibrium chemistry erosion computational results were presented. The differences are striking in that the equilibrium calculation shows much more down bore erosion than the nonequilibrium calculation and also is limited near the forcing cone by the control volume description. The nonequilibrium calculations show a larger influence of the reaction temperature than the equilibrium results when comparing tantalum to chromium. Tantalum may have more erosion than chromium under similar circumstances due to its physical properties.

The dissociation of CO is important and ways to mitigate it were investigated through a review of the literature. Ponec and Barneveld, [21] provided a clue that nitrogen or nitriding the surface may inhibit this dissociation. Experimentally this inhibition of CO dissociation may have been observed by Leveritt, Conroy, and Johnson [22] in new high energetic propellants.

REFERENCES

1. Weinacht, P., and Conroy, P. J., "A Numerical Method for Predicting Thermal Erosion in Gun Tubes," ARL-TR-1156, APG, MD, July 1996.
2. Conroy, P. J., Weinacht, P., and Nusca, M.J., "120-mm Gun Tube Erosion Including Surface Chemistry Effects," US ARL-TR-1526, ARL, APG, MD, 6 October 1997.
3. Conroy, P.J., Weinacht, P., Nusca, M. J., Rice, K., " Analytical Thermal and Erosion Investigation of the Extended Range 5" Navy Gun," Proceedings of 35th JANNAF Combustion Subcommittee Meeting, Tucson, AZ, December 1998.
4. Conroy, P.J., Weinacht, P., Nusca, M. J., "Erosion: A Parametric Study - Flame Temperature," US ARL-TR-1954, June 1999.
5. Conroy, P.J., Weinacht, P., Nusca, M. J., "Gun Tube Coatings in Distress," Proceedings of 36th JANNAF Combustion Subcommittee Meeting, Cocoa Beach, FL, October 1999.
6. Gerber, N., Bundy, M. L., "A Gun Barrel Heating Model that Includes Heat Input During Projectile Passage," ARL-TR-439, APG, MD, June 1994.
7. Ward, J.R., Brosseau, T. L., Kaste, R. P., Stobie, I. C., Bensinger, B., "Erosivity of LOVA Propellants," ARBRL-TR-02368, APG, MD, September 1981.
8. Jones, R.N., Breitbart, S., "A Thermal Theory for Erosion of Guns by Powder Gases," U.S. Army Ballistic Research Laboratories Report No. 747, Aberdeen Proving Ground, MD, January 1959.
9. Frankle, J.M., Kruse, L.R., "A Method for Estimating the Service Life of a Gun or Howitzer," U.S. Army Ballistic Research Laboratories Memorandum Report No. 1852, Aberdeen Proving Ground, MD, June 1967.
10. Lawton, B., "thermal and Chemical Effects on Gun Barrel Erosion," Proceedings of the 10th International Symposium on Ballistics, Orlando FL, October 1984.
11. Anderson, J.D., Hypersonic + High Temperature Gas Dynamics, McGraw Hill, NY, NY, 1989.
12. Nusca, M.J., "Numerical Simulation of Electromagnetic Wave Attenuation in Nonequilibrium chemically Reacting Flows," *Computers and Fluids*, Vol. 27, No. 2, pp.217-238, 1998.
13. Nusca, M.J., Dinavahi, S.P.G., and Soni, B., "Grid Adaptation Studies for Reactive Flow Modeling of Propulsion Systems," AIAA Paper 99-0970, Jan. 1999.
14. Nusca, M.J., McQuaid, M.J., and Anderson, W.R., "Numerical Simulation of an Open-Air Plasma Jet Using a Multi-Species Reacting Flow CFD Code," AIAA 2000-2675, June 2000.
15. Gordon, S., and McBride, B.J., "Computer Program for Calculation of Complex Chemical Equilibrium Compositions, Rocket Performance, Incident and Reflected Shocks, and Chapman-Jouget Detonations," NASA SP-273, NASA Lewis, Cleveland, OH, 1971.
16. Tsang, W., Hampson, R. F., "Chemical Kinetic Database for Combustion Chemistry Part 1. Methane and Related Compounds," Journal of Physical Chemistry Reference Data 15 , 1087, 1986.
17. Grabke, H. J., "Kinetics of the Oxygen Transfer from Carbon Dioxide to the Surface of Iron," Proceedings of the Third International Congress on Catalysis, Vol 2, pp. 928-938, Amsterdam, July 1964.
18. Baulch, D.L., Cobos, C. J., Cox, C. A., Esser, C., Frank, P., Just, Th., Kerr, J. A., Pilling, M. J., Troe, J., Walker, R. W., Warnatz, J., " Evaluated Kinetic Data for Combustion Modeling," Journal of Physical Chemistry Reference Data 21 , pp. 411-429, 1992.
19. Hubbard, C., Gilley, R., Bore Scope Records, Aberdeen Test Center, 1998.
    Ward, J.R., Brosseau, T.L., "Role of the Insulating Layer from TiO_2-Wax Liner in Reducing Gun Tube Wear,"ARBRL-TR-02238, Ballistic Research Laboratory, APG, MD, April, 1980.
20. Cote, P.J., Rickard, C., "Gas Metal Reaction Products in the Erosion of Chromium Plated Gun Bores," Wear, Volume 241, Issue 1, pp. 17-25, June 2000.
21. Ponec, V., van Barneveld, W. A., "The Role of Chemisorption in Fischer-Tropsch Synthesis," Journal of Industrial Engineering Chemical Product Research and Development, Vol. 18, No. 4, 1979.
22. Leveritt, C. S., Johnson, A. J., Conroy, P.J., "Characterization of the Erosivity of Advanced Solid Gun Propellants," Proceedings of 37th JANNAF Combustion Subcommittee Meeting, Monterey, CA, November 2000.